VIP Graphene-Based Nanosheets

DOI: 10.1002/anie.201001634

Graphene-Based Nanosheets with a Sandwich Structure**

Shubin Yang, Xinliang Feng, Long Wang, Kun Tang, Joachim Maier, and Klaus Müllen**

Two-dimensional (2D) nanomaterials, which possess nanoscale dimension in thickness only and infinite length in the plane, have attracted tremendous attention owing to their unique properties and potential applications in the areas of electronics[1] and sensors[2] as well as energy storage[3] and conversion.[4] In particular, recent investigations of graphene, a 2D "aromatic" monolayer of carbon atoms, have demonstrated exceptional physical properties, including ultrahigh electron mobility,[5] ballistic charge carrier transport,[6] and other properties.[7] These studies have triggered wide interest in 2D nanosheets other than carbon, such as transition metal chalcogenides,[8] perovskites,[9] and manganese oxide[10] nanosheets. Unfortunately, in most cases, the above nanosheets have been generated from delamination of their materials with layered structures, and thus the product yields are extremely low owing to the limitations of the fabrication method adopted.[11] This constitutes a major obstacle for exploiting the proposed applications. Therefore, high-throughput production of various 2D nanosheets remains a great challenge. Herein we present a bottom-up approach to the large-scale production of 2D sandwichlike graphene-based mesoporous silica (GM-silica) sheets in which each graphene sheet is fully separated by a mesoporous silica shell. The resulting GM-silica sheets possess a large aspect ratio, mesoporous structure, high surface area, and high monodispersity. Such unique features not only facilitate the diffusion of guest ions or molecules in many diffusion-controlled systems, but also render GM-silica sheets a promising universal template for the creation of various functional sheets, such as graphene-based mesoporous carbon, metal, and metal oxide nanosheets, in which graphene is individually dispersed. We expect that our strategy will be applied to a variety of 2D nanosheet materials to promote their broad applications across the ranges of catalysis, sensors, supercapacitors, and batteries.

2D nanomaterials, and especially nanosheets, have long been considered attractive materials owing to their unique properties and promising applications.[12] Very recently, the single-atom-thick graphene oxide sheets with ultrahigh surface area (2630 $m^2 g^{-1}$ from theoretical calculation based on a single-layer graphene sheet[4]) have been produced by the Hummers method.[13] In contrast to pristine graphite, graphene oxide is heavily oxygenated, bearing hydroxy and epoxide functional groups on their basal planes, along with carbonyl and carboxyl units located at the sheet edges.[14,15] The presence of these oxygen-functionalized groups renders graphene oxide sheets negatively charged. Their zeta potential can reach −43 mV when the pH value of the solution approaches 10.[16] Such unique properties qualify graphene oxide as a reliable and economically feasible source for the production of other 2D nanosheets with ultrahigh surface area. Although this application of graphene oxide is easy to imagine, the actual operation is difficult owing to the intrinsic incompatibility between graphene oxide and inorganic materials.[17] In this work, cationic surfactants, such as cetyltrimethyl ammonium bromide (CTAB), were chosen to electrostatically adsorb and self-assemble onto the surface of highly negatively charged graphene oxide in alkaline solution. This process directs the formation of mesoporous silica around the surface of single-layer graphene oxide (Figure 1a). The utilization of suitable cationic surfactants in our approach not only effectively solves the incompatibility and aggregation problems between graphene oxide and inorganic materials, but also provides the molecular template for controlled nucleation and growth of mesoporous silica on the surface of

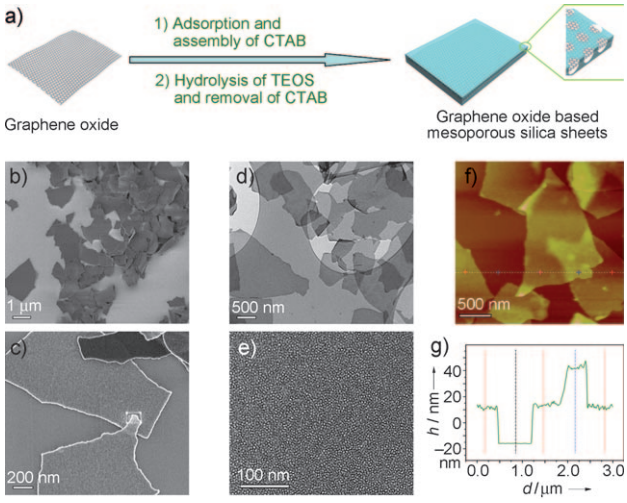

Figure 1. Graphene oxide based mesoporous silica (GOM-silica) sheets. a) Fabrication process for GOM-silica sheets. b,c) Typical FE-SEM and d,e) TEM images reveal the flat GOM-silica sheets with sizes from 200 nm to several micrometers and having a mesoporous structure. f) Representative AFM image and g) corresponding thickness analysis taken around the white line in (f) reveal a uniform thickness of 28 nm for GOM-silica sheets.

[*] Dr. S. Yang, Dr. X. Feng, Dr. L. Wang, Prof. Dr. K. Müllen
Max-Planck-Institut für Polymerforschung
Ackermannweg 10, 55128 Mainz (Germany)
Fax: (+49) 6131-379-350
E-mail: feng@mpip-mainz.mpg.de
muellen@mpip-mainz.mpg.de
Dr. K. Tang, Prof. Dr. J. Maier
Max-Planck-Institut für Festkörperforschung
Heisenbergstrasse 1, 70569 Stuttgart (Germany)

[**] This work was financially supported by the Max Planck Society through the program ENERCHEM, the German Science Foundation (Korean–German IRTG) and the DFG Priority Program SPP 1355.

Supporting information for this article is available on the WWW under http://dx.doi.org/10.1002/anie.201001634.

graphene oxide sheets. By this means, 2D sandwichlike graphene oxide-based mesoporous silica (GOM-silica) sheets are constructed. Upon thermal treatment of GOM-silica sheets at high temperature, graphene oxide can be reduced to individual graphene without aggregation owing to the perfect protection of silica, and at the same time gives birth to the GM-silica sheets. It thus opens up a unique opportunity for the large-scale production of various functional nanosheets, such as mesoporous carbon, metal, and metal oxide sheets with or without graphene.

First, the morphology and microstructure of as-prepared GOM-silica sheets were investigated by field emission scanning electron microscopy (FE-SEM) and transmission electron microscopy (TEM). As shown in Figure 1 b–d, many free-standing sheets with morphology similar to that of graphene and with sizes ranging from 200 nm to several micrometers are observed. Remarkably, the resulting sheets possess numerous mesopores with the size of about 2 nm (Figure 1 e; Supporting Information, Figure S1); no free silica particles or naked graphene oxide sheets appear in either TEM or SEM visualizations. This result suggests that, as expected, most of the surfactants are concentrated on the surface of graphene oxide by electrostatic interactions, thus facilitating the heterogeneous nucleation process of tetraethyl orthosilicate (TEOS) around the surface of graphene oxide rather than a homogeneous nucleation process in bulk solution. Once the silica nucleation occurs, the residual TEOS can further hydrolyze and grow around the silica nucleus on the surface of graphene oxide according to the well-known liquid-crystal template mechanism.[18] As a result, the mesoporous silica is homogenously coated on the surface of graphene oxide sheets. The nature of the structure can be further unraveled by the element mapping images of carbon, silicon, and oxygen in the GOM-silica sheets (Figure 2), in agreement with energy-dispersive X-ray (EDX) analysis (Supporting Information, Figure S2). With such a synthetic procedure, it can also be expected that graphene-based nanosheets with ordered mesoporous structure should be achieved, which shall offer additional functionality.[19–21] Furthermore, the as-prepared GOM-silica sheets are highly transparent to electron beams, as shown in the TEM image (Figure 1 d), indicating possible applications in optical devices.[22] Cross-sectional atomic force microscopy (AFM) analyses were conducted to further investigate the structural features of GOM-silica sheets. Their typical AFM image and thickness analyses (Figure 1 f and g) reveal the same morphology as the observations from SEM and TEM, with a uniform thickness of 28 ± 1 nm. Notably, the thickness of the sheets is readily tunable by simply adjusting the ratio of graphene oxide to TEOS in the fabrication process.

It is well-known that graphene oxide is an electrically insulating material, which arises from the presence of large amounts of oxygen functional groups on their basal planes. Upon removal of such species, the electronic properties of graphene sheets are supposed to be restored.[23–26] Several reduction procedures of graphene oxide, including chemical, thermal, and ultraviolet-assisted reduction, have recently been proposed.[23–26] However, these reduction processes commonly suffer from the irreversible aggregation of graphene originating from the strong π interactions, which significantly prevents their further applications. In contrast, simple pyrolysis of as-prepared GOM-silica sheets in our approach can effectively reduce graphene oxide to graphene without aggregation owing to the perfect protection of silica. This feature is indeed demonstrated by the SEM and TEM images of graphene after removal of silica (Supporting Information, Figure S3). Remarkably enough, pyrolysis yields GM-silica sheets in which the graphene is individually dispersed and the content is about 12%, as calculated by EDX (Figure 3 c) and thermogravimetric analysis (Supporting Information, Figure S4). The morphology and structure of GM-silica sheets are quite stable during the heat treatment, as the same flat shape and mesoporous structure with respect to those of the sample before pyrolysis are seen (Figure 3 a,b).

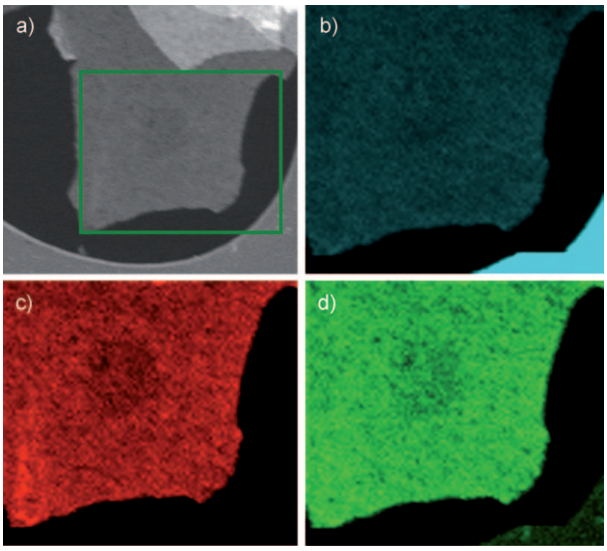

Figure 2. Elemental mapping images of GOM-silica sheets. a) Typical scanning transmission electron microscopy (STEM) image and corresponding elemental mapping images of b) carbon, c) silicon, and d) oxygen in the selected area (blue rectangle in (a)), indicating the homogeneous dispersion of C, Si, and O in GOM-silica sheets.

The mesoporous nature of GM-silica sheets is further confirmed by nitrogen physisorption measurements. Their adsorption–desorption isotherm exhibits a type IV nitrogen adsorption branch associated with a well-defined capillary condensation step at about 0.25 P/P_0, which is characteristic of uniform mesopores (Figure 3 d). The pore size distribution calculated by the Barrett–Joyner–Halenda (BJH) method is 2 nm (inset in Figure 3 d), which is in good agreement with the pore size estimated from the TEM images. The very small hysteresis between the adsorption and desorption branches (at 0.4–0.8 P/P_0) further suggests a highly uniform pore size with no pore-blocking effects from narrow pores during desorption. Furthermore, the adsorption data indicate a very high specific surface area of 980 $m^2 g^{-1}$, which is comparable to the values reported for conventional mesoporous silica.[27] Thus, the high specific surface area, large aspect ratio, and high production yield (Supporting Information, Figure S5) render GM-silica sheets a promising template for generating various functional nanosheets. For typical examples, we have

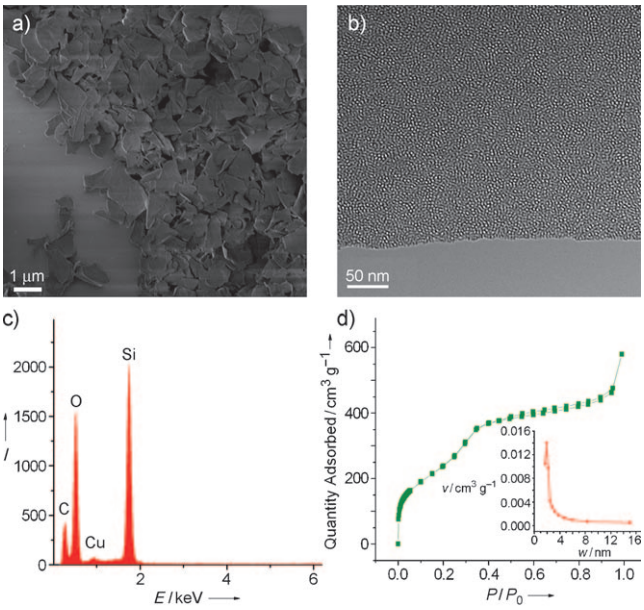

Figure 3. Graphene-based mesoporous silica (GM-silica) sheets after pyrolysis at 800 °C. a) FE-SEM and b) TEM images reveal the stable morphology and mesoporous structure of GM-silica sheets after pyrolysis at high temperature. c) EDX spectrum, suggesting that graphene remains in GM-silica sheets. d) Nitrogen adsorption/desorption isotherm of graphene–mesoporous silica sheets (inset: pore size distribution), further demonstrating the mesoporous structure, with the pore size of 2 nm and BET surface area of 980 $m^2 g^{-1}$.

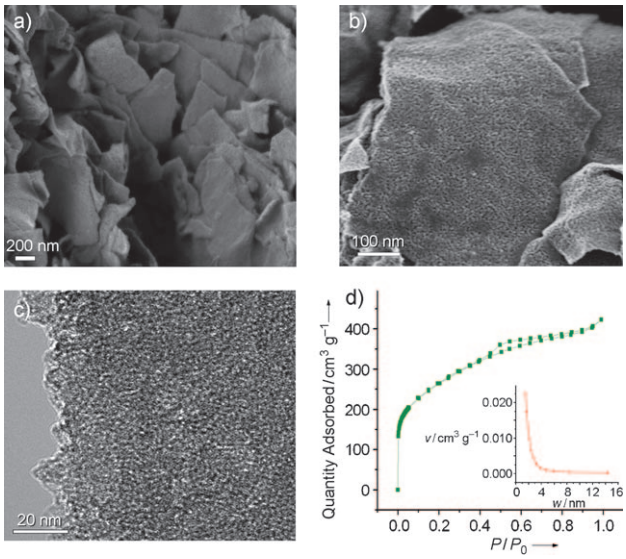

Figure 4. Graphene-based mesoporous carbon (GM-C) sheets derived from GM-silica sheets. a,b) FE-SEM, c) HRTEM images, and d) nitrogen adsorption/desorption isotherm of GM-C sheets disclosing their flat shape and porous structure. Inset in (d): pore size distribution.

employed the GM-silica sheets as a template, with sucrose as carbon source and cobalt nitrate as cobalt source, to fabricate graphene-based mesoporous carbon (GM-C) and Co_3O_4 (GM-Co_3O_4) sheets, respectively, by a simple nanocasting approach. The pronounced electrochemical properties of GM-C as an anode material for lithium ion batteries will be evaluated below.

The electron microscopy images of GM-C and GM-Co_3O_4 sheets derived from the graphene-based mesoporous silica sheets are presented in Figure 4 (see also the Supporting Information, Figures S6 and S7). In the case of GM-C sheets, although twisted sheets could be observed, which was possibly caused by the shrinkage of the sample during thermal treatment, most sheets maintain their large aspect ratio. Furthermore, GM-C sheets exhibit high monodispersity with the same size as the template (Figure 4a). These obviously originate from the perfect replication of the structure and morphology of GM-silica sheets. Cross-sectional FE-SEM and high-resolution transmission electron microscopy (HRTEM) images (Figure 4b and c) in association with the X-ray diffraction (XRD) pattern (Supporting Information, Figure S8) reveal the porous and amorphous structures in GM-C sheets. A high Brunauer–Emmett–Teller (BET) surface area of up to 910 $m^2 g^{-1}$ has been obtained based on the nitrogen adsorption–desorption analysis. The type IV isotherm with pronounced adsorptions at low (< 0.1 P/P_0) and medium (0.2–0.8 P/P_0) relative pressures (Figure 4d) indicate the existence of a large number of mesopores and micropores in GM-C sheets. This is a result of the replication of the mesoporous template and continuous decomposition of the carbon source during the pyrolysis process. For comparison, GM-Co_3O_4 sheets possess mesoporous but crystalline structures (Supporting Information, Figure S7–S9). Single crystals in the individual spherical domains and polycrystals in the whole GM-Co_3O_4 sheets are visible in the typical HRTEM image (Supporting Information, Figure S7c). This arises from the seed formation mechanism of Co_3O_4 in the pores of the template; that is, the Co_3O_4 seeds are firstly randomly formed in the pores of mesoporous silica, and then amorphous Co_3O_4 starts to grow around the seeds during the thermolysis process.[27] The presence of graphene in such GM-Co_3O_4 sheets was confirmed by EDX analysis (Supporting Information, Figure S7d), indicating that the individually dispersed graphene in the template has been successfully transferred to the new nanosheets during our casting process. Apparently, this strategy could be further extended to fabricate a variety of mesoporous metal and metal oxide sheets made, for example, from Sn, SnO_2, TiO_2, and MnO_2 with or without graphene. To the best of our knowledge, mesoporous carbon, metal, and metal oxide sheets with such thin thickness, large aspect ratio, and high surface area have never been reported. Clearly, such unique features for 2D nanomaterials hold great promise for new functions with respect to the traditional mesoporous nanomaterials.

One promising application of these 2D nanosheets can be envisioned in the context of lithium ion storage. Their high surface area, thinness, and numerous mesopores will be favorable for the accessibility of the electrolyte, rapid diffusion of lithium ions, and host uptake. Furthermore, the graphene layers within each nanosheet can act as mini-current collectors homogeneously dispersed in the electrode, which will facilitate the fast transport of electrons during the charge–discharge processes owing to the high electrical conductivity of graphene (Figure 5a). Thus, GM-C sheets were chosen to evaluate their lithium ion storage properties

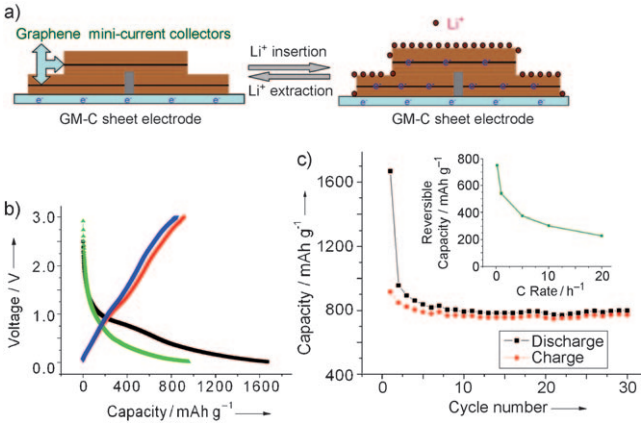

Figure 5. Electrochemical performance of GM-C sheets for lithium ion storage. a) Lithium insertion and extraction in GM-C sheets, where graphene acts as mini-current collectors during discharge and charge processes, facilitating the rapid diffusion of electrons during cycling processes. b) First two discharge–charge curves (■ first discharge, ● first charge, ▲ second discharge, ▼ second charge) and c) cycle performance (■ discharge, ● charge) of GM-C sheets at a rate of C/5. The inset in (c) is the rate capability of GM-C sheets at various rates of C/5, 1C, 5C, 10C, and 20C.

by galvanostatic discharge (lithium insertion)–charge (lithium extraction) measurements. It is remarkable to note a very high first reversible capacity (915 mAh g^{-1}) at a rate of C/5 (one lithium per six formula units (LiC_6) in 5 h), corresponding to an extraction of 2.5 mol of lithium ions per 6 mol of carbon ($Li_{2.5}C_6$; Figure 5b). After 30 cycles, both discharge and charge capacities of GM-C sheets are stabilized at about 770 mAh g^{-1}, delivering 84% capacity retention. Moreover, GM-C sheets exhibit excellent rate performance. For example, when the discharge–charge rates are increased to 1C and 5C, the reversible capacities are as high as 540 and 370 mAh g^{-1}, respectively (Figure 5c). This result is in stark contrast to the traditional non-graphitic carbons, which show continuous and progressive capacity decay along with cycling processes,[28–30] and it is even better than the porous graphitic carbons.[31,32] As a consequence, the results obtained herein give clear evidence that the utility of graphene-based nanosheets can significantly improve the electrochemical performance owing to their favorable structures, as discussed above. Our bottom-up synthetic approach will certainly be utilized to explore further functional 2D nanomaterials, with applications in catalysis, sensors, supercapacitors, batteries, and fuel cells.

Experimental Section

Graphene oxide was synthesized from natural graphite flakes by a modified Hummers method.[13] Graphene oxide based mesoporous silica sheets were prepared by electrostatic interaction between negatively charged graphene oxide and cationic surfactant and the self-assembly of surfactant. In a typical experiment, as-synthesized graphene oxide (30 mg) was firstly suspended in an aqueous solution containing CTAB (1 g) and NaOH (40 mg), and then ultrasonically treated for 3 h. After magnetic stirring for 2 h at 40 °C, tetraethylorthosilicate (TEOS, 1 mL) was slowly added to the above mixture. After reaction for 12 h, the desired graphene oxide based mesoporous silica sheets were obtained by washing with warm ethanol, separation, and drying. Graphene-based mesoporous silica sheets were produced by pyrolysis of graphene oxide based mesoporous silica sheets at 800 °C for 3 h in argon.

Graphene-based mesoporous carbon and Co_3O_4 sheets were prepared using graphene-based mesoporous silica sheets as a template by a nanocasting approach. Typically, an ethanol solution of sucrose or cobalt nitrate was repeatedly impregnated into the template under magnetic stirring at 40 °C, where the weight ratios between sucrose and template or cobalt nitrate and template were fixed to 2:1 or 2.3:1, respectively. Later on, the sucrose-filled template was pyrolyzed at 700 °C for 3 h in argon, and the template filled with cobalt nitrate was treated at 350 °C for 5 h in air. Subsequent etching of the resulting samples in a NaOH solution gave birth to graphene-based mesoporous carbon and Co_3O_4 sheets.

The morphology and microstructure of the samples were investigated by FE-SEM (Hitachi SU8000), TEM (Philips EM 420), HRTEM (Philips Tecnai F20), STEM (Philips Tecnai F20), AFM (Veeco Dimension 3100), EDX (Philips Tecnai F20), SAED (Philips Tecnai F20), and TGA (Mettler TG 50) measurements. Nitrogen sorption isotherms and BET surface area were measured at 77 K with a Micromeritcs Tristar 3000 analyzer (USA). Electrochemical experiments were carried out in 2032 coin-type cells. The working electrodes were prepared by mixing GM-C, carbon black (Super-P), and poly(vinyl difluoride) (PVDF) at a weight ratio of 80:10:10 and pasted on pure copper foil (99.6%, Goodfellow). Pure lithium foil (Aldrich) was used as the counter electrode. The electrolyte consisted of a solution of 1M $LiPF_6$ in ethylene carbonate (EC)/dimethyl carbonate (DMC) (1:1 by volume) obtained from Ube Industries Ltd. The cells were assembled in an argon-filled glovebox with the concentrations of moisture and oxygen below 1 ppm. The electrochemical performance was tested at various rates in the voltage range of 0.01–3.00 V.

Received: March 18, 2010
Published online: May 28, 2010

Keywords: electrochemistry · graphene · nanosheets · nanostructures

[1] K. S. Novoselov, Z. Jiang, Y. Zhang, S. V. Morozov, H. L. Stormer, U. Zeitler, J. C. Maan, G. S. Boebinger, P. Kim, A. K. Geim, *Science* **2007**, *315*, 1379.
[2] F. Schedin, A. K. Geim, S. V. Morozov, E. W. Hill, P. Blake, M. I. Katsnelson, K. S. Novoselov, *Nat. Mater.* **2007**, *6*, 652.
[3] J. W. Seo, Y. W. Jun, S. W. Park, H. Nah, T. Moon, B. Park, J. G. Kim, Y. J. Kim, J. Cheon, *Angew. Chem.* **2007**, *119*, 8984; *Angew. Chem. Int. Ed.* **2007**, *46*, 8828.
[4] M. D. Stoller, S. J. Park, Y. W. Zhu, J. H. An, R. S. Ruoff, *Nano Lett.* **2008**, *8*, 3498.
[5] A. K. Geim, *Science* **2009**, *324*, 1530.
[6] X. Du, I. Skachko, A. Barker, E. Y. Andrei, *Nat. Nanotechnol.* **2008**, *3*, 491.
[7] X. L. Li, X. R. Wang, L. Zhang, S. W. Lee, H. J. Dai, *Science* **2008**, *319*, 1229.
[8] J. W. Seo, J. T. Jang, S. W. Park, C. J. Kim, B. W. Park, J. W. Cheon, *Adv. Mater.* **2008**, *20*, 4269.
[9] M. Osada, T. Sasaki, *J. Mater. Chem.* **2009**, *19*, 2503.
[10] Y. Omomo, T. Sasaki, L. Z. Wang, M. Watanabe, *J. Am. Chem. Soc.* **2003**, *125*, 3568.
[11] J. S. Son, X. D. Wen, J. Joo, J. Chae, S. I. Baek, K. Park, J. H. Kim, K. An, J. H. Yu, S. G. Kwon, S. H. Choi, Z. W. Wang, Y. W. Kim, Y. Kuk, R. Hoffmann, T. Hyeon, *Angew. Chem.* **2009**, *121*, 6993; *Angew. Chem. Int. Ed.* **2009**, *48*, 6861.
[12] W. M. R. Divigalpitiya, R. F. Frindt, S. R. Morrison, *Science* **1989**, *246*, 369.

[13] W. S. Hummers, R. E. Offeman, *J. Am. Chem. Soc.* **1958**, *80*, 1339.
[14] H. Y. He, J. Klinowski, M. Forster, A. Lerf, *Chem. Phys. Lett.* **1998**, *287*, 53.
[15] S. Stankovich, D. A. Dikin, G. H. B. Dommett, K. M. Kohlhaas, E. J. Zimney, E. A. Stach, R. D. Piner, S. T. Nguyen, R. S. Ruoff, *Nature* **2006**, *442*, 282.
[16] D. Li, M. B. Müller, S. Gilje, R. B. Kaner, G. G. Wallace, *Nat. Nanotechnol.* **2008**, *3*, 101.
[17] D. H. Wang, D. W. Choi, J. Li, Z. G. Yang, Z. M. Nie, R. Kou, D. H. Hu, C. M. Wang, L. V. Saraf, J. G. Zhang, I. A. Aksay, J. Liu, *Acs Nano* **2009**, *3*, 907.
[18] G. S. Attard, J. C. Glyde, C. G. Goltner, *Nature* **1995**, *378*, 366.
[19] I. A. Aksay, M. Trau, S. Manne, I. Honma, N. Yao, L. Zhou, P. Fenter, P. M. Eisenberger, S. M. Gruner, *Science* **1996**, *273*, 892.
[20] H. Yang, A. Kuperman, N. Coombs, S. MamicheAfara, G. A. Ozin, *Nature* **1996**, *379*, 703.
[21] H. Yang, N. Coombs, I. Sokolov, G. A. Ozin, *Nature* **1996**, *381*, 589.
[22] S. Watcharotone, D. A. Dikin, S. Stankovich, R. Piner, I. Jung, G. H. B. Dommett, G. Evmenenko, S. E. Wu, S. F. Chen, C. P. Liu, S. T. Nguyen, R. S. Ruoff, *Nano Lett.* **2007**, *7*, 1888.
[23] S. Park, R. S. Ruoff, *Nat. Nanotechnol.* **2009**, *4*, 217.
[24] S. Stankovich, D. A. Dikin, R. D. Piner, K. A. Kohlhaas, A. Kleinhammes, Y. Jia, Y. Wu, S. T. Nguyen, R. S. Ruoff, *Carbon* **2007**, *45*, 1558.
[25] D. R. Dreyer, S. Park, C. W. Bielawski, R. S. Ruoff, *Chem. Soc. Rev.* **2010**, *39*, 228.
[26] D. V. Kosynkin, A. L. Higginbotham, A. Sinitskii, J. R. Lomeda, A. Dimiev, B. K. Price, J. M. Tour, *Nature* **2009**, *458*, 872.
[27] C. Dickinson, W. Z. Zhou, R. P. Hodgkins, Y. F. Shi, D. Y. Zhao, H. Y. He, *Chem. Mater.* **2006**, *18*, 3088.
[28] J. R. Dahn, T. Zheng, Y. H. Liu, J. S. Xue, *Science* **1995**, *270*, 590.
[29] S. B. Yang, X. L. Feng, L. J. Zhi, Q. Cao, J. Maier, K. Müllen, *Adv. Mater.* **2010**, *22*, 838.
[30] S. B. Yang, G. L. Cui, S. P. Pang, Q. Cao, U. Kolb, X. L. Feng, J. Maier, K. Müllen, *ChemSusChem* **2010**, *3*, 236.
[31] N. A. Kaskhedikar, J. Maier, *Adv. Mater.* **2009**, *21*, 2664.
[32] P. Adelhelm, Y. S. Hu, L. Chuenchom, M. Antonietti, B. M. Smarsly, J. Maier, *Adv. Mater.* **2007**, *19*, 4012.

